Cell Reports Medicine, Volume *1*

Supplemental Information

Single-Cell Analyses Identify Dysfunctional $CD16^{+}$ CD8 T Cells in Smokers

Suzanne N. Martos, Michelle R. Campbell, Oswaldo A. Lozoya, Xuting Wang, Brian D. Bennett, Isabel J.B. Thompson, Ma Wan, Gary S. Pittman, and Douglas A. Bell

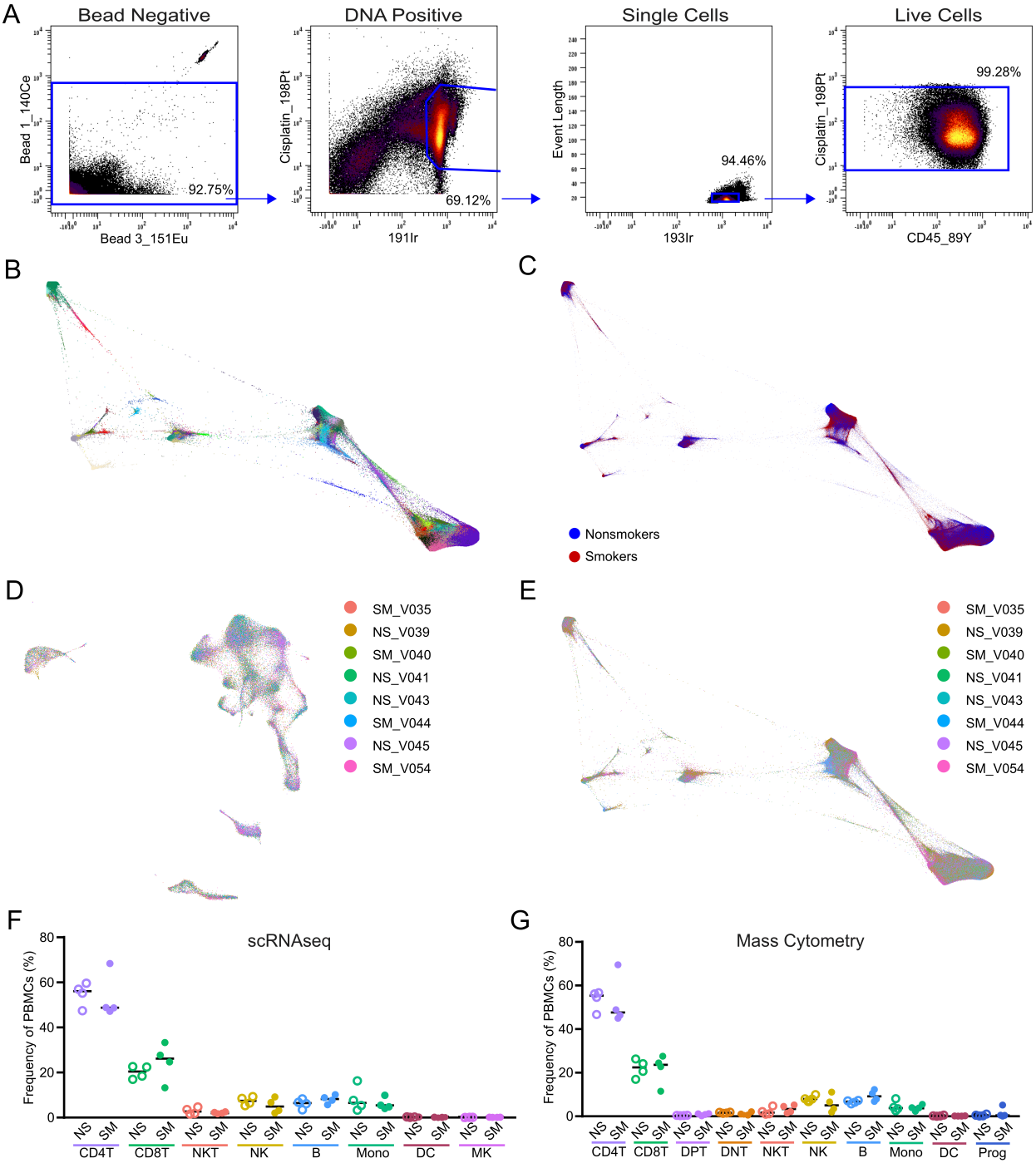

Figure S1. scRNAseq and mass cytometry profiling of PBMCs, Related to Figure 1. (A) Mass cytometry biaxial plots of the gating strategy. Cells gated from spiked-in normalization beads are subsequently gated by Iridium (191Ir) and Cisplatin (198Pt) to obtain DNA positive cells. Single cells are identified by event length and Iridium (193Ir) and viable cells by Cisplatin-198Pt and leukocyte marker CD45 (example from a single donor). **(B-C)** FDL mass cytometry (n=8) of 122 immune cell cluster IDs displayed by cluster ID color **(B)** and smoking status (**C**; 4 nonsmokers blue, 4 smokers red). **(D)** scRNAseq UMAP (n=8) as described in **Figure 1B**. Cells are colored by individual donors. **(E)** Mass cytometry FDL as described in **Figure 1C**. Cells are colored by individual donors. **(F-G)** Frequencies of PBMCs by major cells types compared between smokers (filled, n=4) and nonsmokers (unfilled, n=4) for scRNAseq **(F)** or mass cytometry. **(G)** did not show significant differences. Bar = median, Mann-Whitney U test.

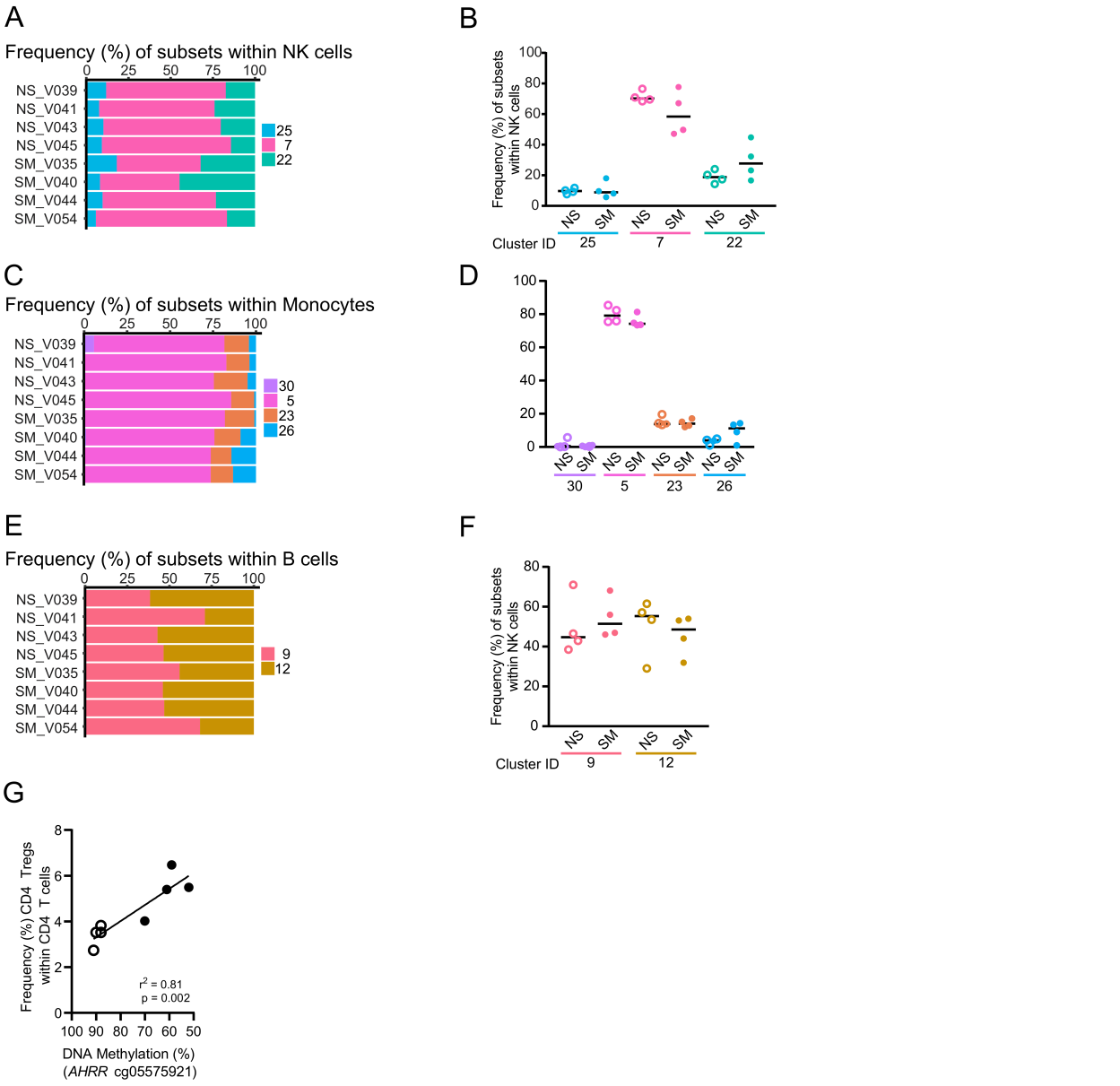

Figure S2. Subtype distributions within other major cell populations do not shift between smokers (SM, n=4) and nonsmokers (NS, n=4), Related to Figure 2. (A-B) Frequency of subsets within NK cells. Individual donor distribution of NK cell subsets **(A)**. Smokers (filled) had no significant shifts in NK cell frequency compared to nonsmokers (unfilled). Bar = median, Mann-Whitney U test **(B)**. **(C-D) Frequency of subsets within monocytes.** Individual donor distribution of monocyte subsets **(C)**. Smokers (filled) had no significant shifts in monocyte frequency compared to nonsmokers (unfilled). Bar = median, Mann-Whitney U test **(D)**. **(E-F) Frequency of subsets within B cells.** Individual donor distribution of B cell subsets **(E)**. Smokers (filled) had no significant shifts in B cell frequency compared to nonsmokers (unfilled). Bar = median, Mann-Whitney U test **(F)**. **(G)** Frequency of CD4 Tregs correlated with smoking dose (reduced *AHRR* DNA methylation).

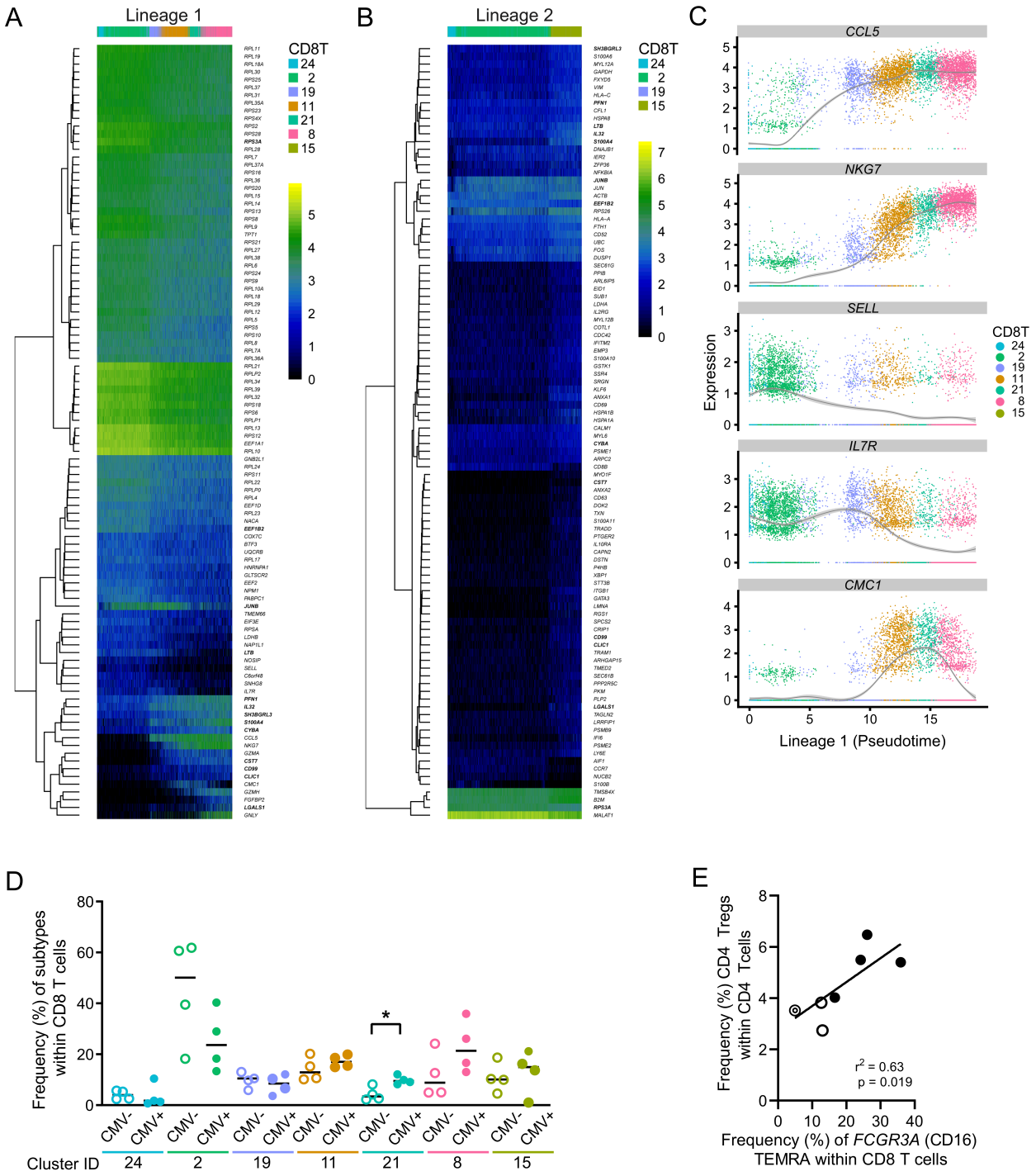

Figure S3. CD8 subsets shift from naïve to differentiated CD8 T cell states, Related to Figure 3.
(A-B) Pseudotemporal heatmaps of CD8 T cell differentiation (n=8) of Lineage 1 **(A)** and Lineage 2 **(B)**.
(C) Pseudotemporal trajectory of CD8 T cell differentiation in Lineage 1 of *CCL5*, *NKG7*, *SELL*, *IL7R* and *CMC1*.
(D) Human cytomegalovirus (HCMV) seropositive (IgG+/IgM-) donors (filled, n=4) had significantly increased frequency of CD8T-21 cells compared to HCMV seronegative (IgG-/IgM-) donors (unfilled, n=4). Bar=median, *p<0.05 by Mann-Whitney U test. **(E)** Frequency of CD4 Tregs correlated with frequency of *FCGR3A* CD8 T_{EMRA} cells.

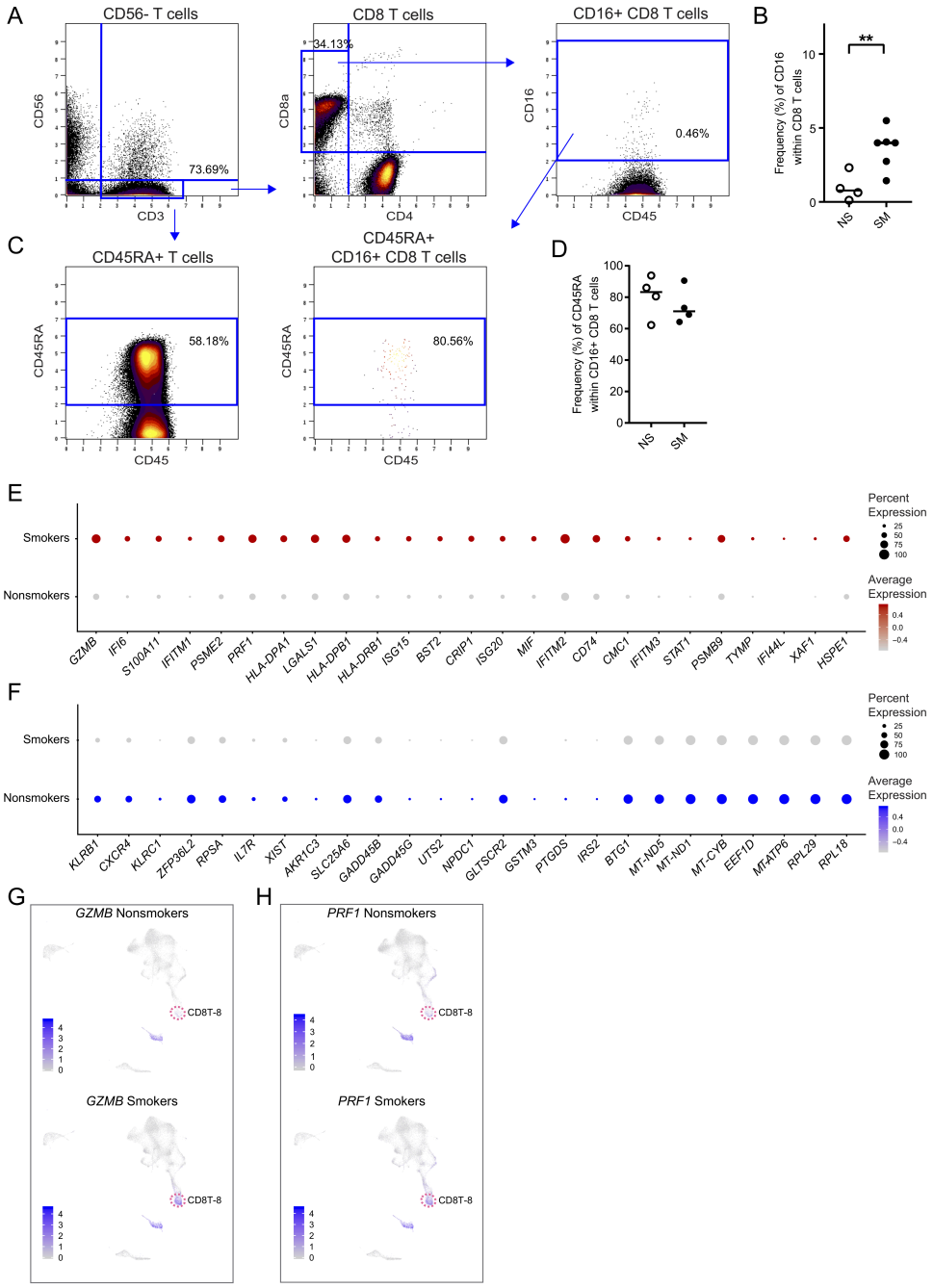

Figure S4. CD16$^+$ CD8 T cells characterization by scRNAseq, Related to Figure 4. (A) Mass cytometry gated to determine frequency of CD16$^+$ CD8 T cells (example from single donor). Viable cells (**Figure S1A**, right panel) in a CD3/CD56 biaxial plot. CD56$^-$ cells (lower right quadrant) gated by CD4 and CD8 to obtain single positive CD8 T cells (upper left quadrant) were used to determine CD16$^+$ CD8 T cell frequency. **(B)** CD16$^+$ cells increased in smokers' CD8 T cells (filled, n=6) compared to nonsmokers (unfilled, n=4) in an independent group of donors. Bar=median, **p<0.01 by one-tailed Mann-Whitney U test. **(C)** CD3$^+$ T cells gated by CD45RA/CD45 to establish CD45RA$^+$ gate and applied to CD16$^+$ CD8 T cells showed the majority were CD45RA positive. **(D)** CD45RA$^+$ cell frequency in CD16$^+$ CD8 T cells from smokers (n=4) and nonsmokers (n=4). Bar = median, Mann-Whitney U test. **(E-F)** Genes altered in smokers in the CD8T-8 subset. 25 genes with increased **(E)** or decreased **(F)** per cell gene expression were ordered by the difference in percentage of CD8T-8 cells expressing each gene between smokers (n=4) and nonsmokers (n=4). Color intensity indicates average per cell expression and circle size represents percent of cells expressing the gene. **(G-H)** UMAP comparison of nonsmokers and smokers, as described in **Figure 4C** and **4E,** displaying the increase in *GZMB* **(G)** and *PRF1* **(H)** from smokers in the CD8T-8 cluster.

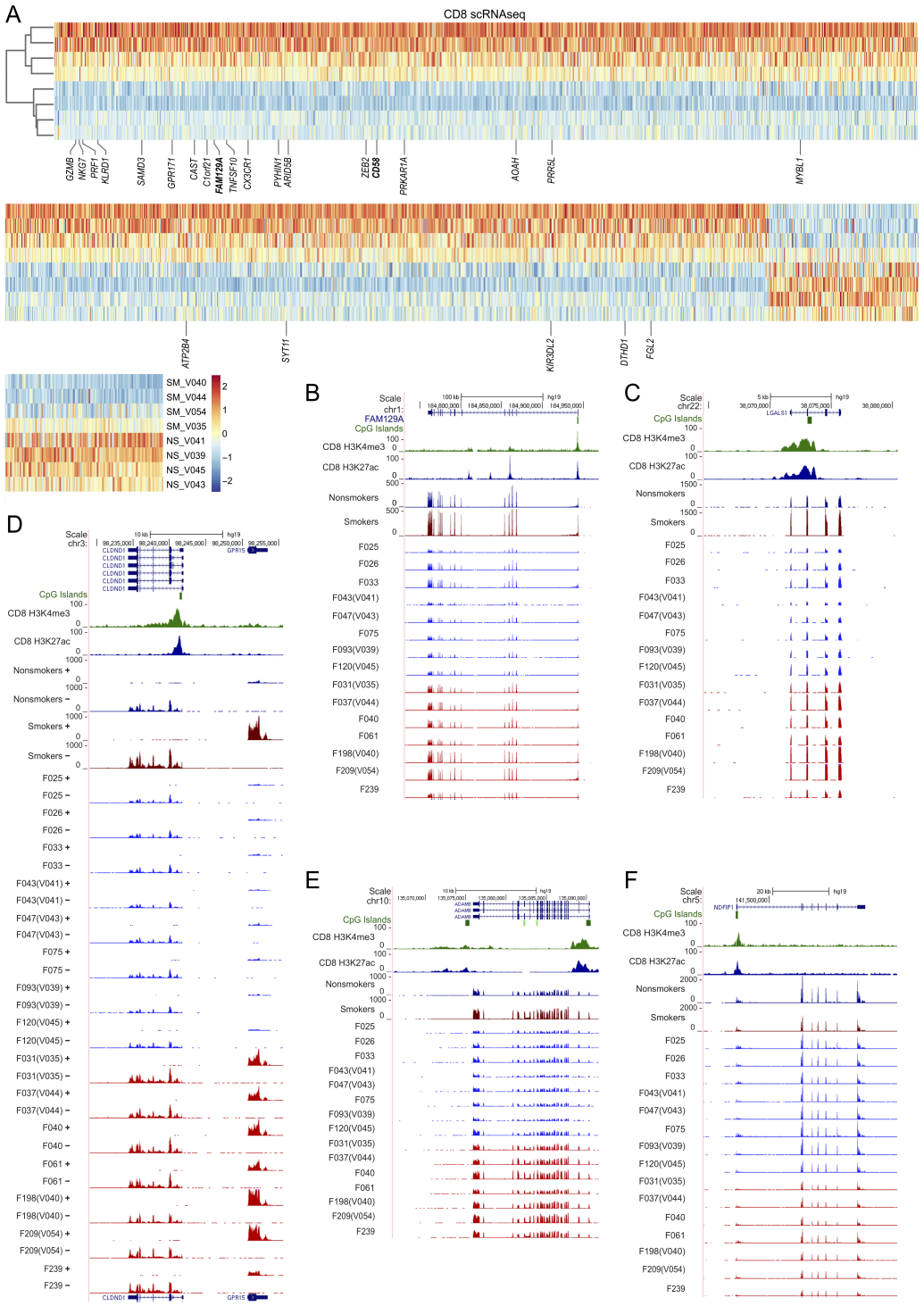

Figure S5. Activation of CD8 T cells in peripheral blood of smokers, Related to Figure 5. (A) scRNAseq heatmap of all differentially expressed genes (DEGs) between smokers (n=4) and nonsmokers (n=4) from seven CD8 T cells clusters. Individual donors were separated by smoking status using smoking scRNA-DEGs for hierarchical clustering. Genes labeled were also found to be significantly upregulated in the CD8 T cell microarray results (See **Figure 5D**). **(B-F) Genome browser tracks of DEGs from bulk RNAseq (n=8 nonsmokers, n=7 smokers).** *FAM129A* was significantly increased by all three platforms **(B)**. *LGALS1* **(C)**, *CLDND1* **(D)**, and *ADAM8* **(E)**, were significantly increased in bulk RNAseq and scRNAseq data, while *GPR15* **(D)** was increased in RNAseq and microarray data. *NDFIP1* **(F)** was significantly decreased in bulk RNAseq and scRNAseq data.

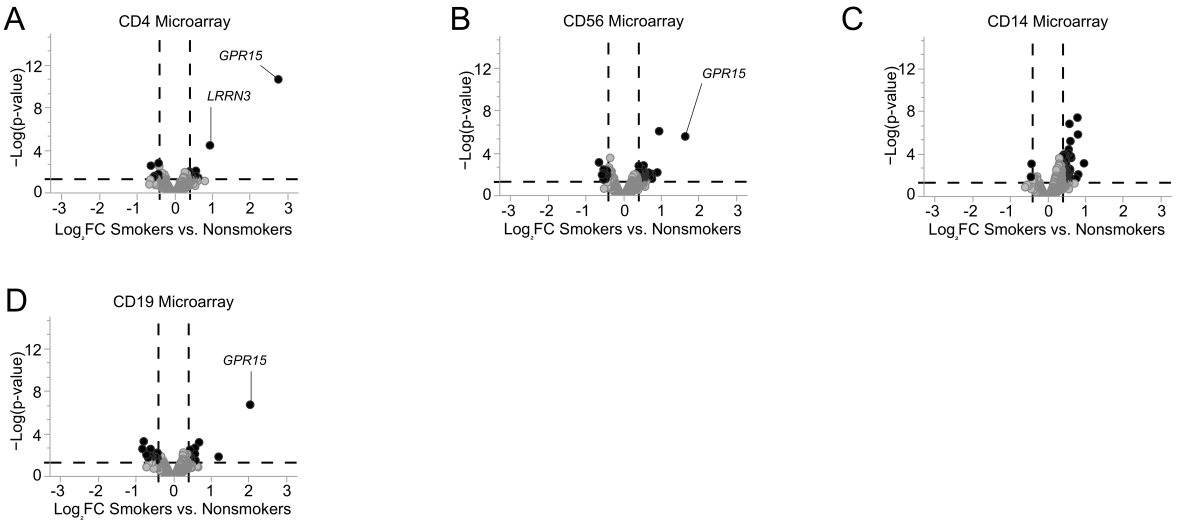

Figure S6. Other major cell type expression changes in peripheral blood of smokers, Related to Figure 6. **(A-D)** Microarray volcano plots of isolated $CD4^+$ T cells **(A,** n=10 nonsmokers, n=9 smokers**)**, $CD56^+$ cells **(B,** n=11 nonsmokers, n=12 smokers**)**, $CD14^+$ cells **(C,** n=10 nonsmokers, n=9 smokers**)** and $CD19^+$ B cells **(D,** n=10 nonsmokers, n=9 smokers**)**.